

Structural Delineation of MDC1-FHA Domain Binding with CHK2-pThr68

Hsin-Hui Wu,^{†,||} Pei-Yu Wu,[†] Kai-Fa Huang,[†] Yu-Ya Kao,[†] and Ming-Daw Tsai^{*,†,||,‡,§}

[†]Institute of Biological Chemistry and [‡]Genomics Research Center, Academia Sinica, Nankang, Taipei 115, Taiwan

[§]Institute of Biochemical Sciences, National Taiwan University, Taipei 10617, Taiwan

^{||}Institute of Bioinformatics and Structure Biology, National Tsing Hua University, Hsinchu 300, Taiwan

Supporting Information

ABSTRACT: Mammalian MDC1 interacts with CHK2 in the regulation of DNA damage-induced S-phase checkpoint and apoptosis, which is directed by the association of MDC1-FHA and CHK2-pThr68. However, different ligand specificities of MDC1-FHA have been reported, and no structure is available. Here we report the crystal structures of MDC1-FHA and its complex with a CHK2 peptide containing pThr68. Unlike other FHA domains, MDC1-FHA exists as an intrinsic dimer in solution and in crystals. Structural and binding analyses support pThr+3 ligand specificity and provide structural insight into MDC1-CHK2 interaction.

The conserved FHA domain of MDC1 was reported to interact with ATM,^{1,2} which presumably controls ATM-dependent intra-S-phase checkpoint, G2/M checkpoint, and radiation-induced apoptosis.³ The binding specificity of MDC1-FHA was reported to be pT-Q-X-I/L in vitro,⁴ which matches the sequence flanking the ATM-phosphorylated Thr68 of CHK2. Indeed, MDC1-FHA regulates CHK2-mediated DDR, leading to S-phase checkpoint and apoptosis.⁵ Although MDC1-FHA binds both ATM and CHK2,^{1,2,5} the latter does not colocalize with MDC1 at IRIF and remains in diffusive patterns in the nucleus,⁶ implying a relatively transient interaction in vivo between MDC1 and CHK2.³ Because most cases of FHA-pThr binding are relatively stable [e.g., NBS1-MDC1-pSDpTD⁷⁻⁹ and RNF8-FHA-MDC1-TQXF¹⁰], the proposed transient binding nature makes the interaction between MDC1-FHA and CHK2-pThr68 an interesting FHA binding mode.

The goal of this work is to characterize the potentially novel binding specificity of MDC1-FHA. We first tried to crystallize human MDC1-FHA (hMDC1-FHA amino acids 16–142, 27–155, and 27–142) and their complexes with a pThr68 peptide derived from human CHK2 (hCHK2-pThr68, LETVSpTQE-LYSI), but without success. Because mouse MDC1 (mMDC1) has been functionally characterized¹ and the level of sequence identity between human and mouse homologues is at least 80% (Figure 1A), we tried to use mMDC1-FHA as the model to deduce the interaction. Analysis by PONDOR (<http://www.pondr.com>) suggested that the ordered region of mMDC1-FHA spans amino acids 29–139 [SI (Supporting Information) Figure 1]. We then synthesized the coding sequence, bacterially expressed the protein, and successfully obtained crystals in the

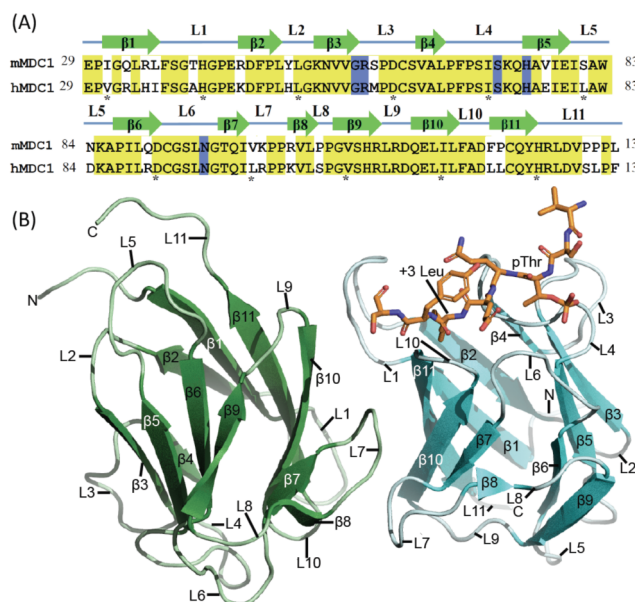


Figure 1. Sequence and structure of mMDC1-FHA. (A) Secondary structure elements according to mMDC1-FHA structures. The identical residues of the mouse and human sequences are highlighted in yellow and the conserved residues of the FHA domain in blue. The UniProt accession numbers of both sequences are Q5PSV9 (mouse MDC1) and Q14676 (human MDC1). (B) Ribbon diagram of the complex structure of the mMDC1-FHA dimer and CHK2-pThr68 peptide. The left and right panels show the structures of chain A (green) and chain B (cyan) of mMDC1-FHA, respectively. The CHK2-pThr68 peptide in the complex structure is shown as orange sticks.

presence and absence of the hCHK2-pT68 peptide (sequence identical to that of mouse CHK2 except +4 Cys).

The complex crystallized in space group $P2_12_12_1$, with two copies of mMDC1-FHA and one hCHK2-pThr68 peptide in an asymmetric unit (Figure 1B). The structure of the complex was determined by the SAD phasing method using diffraction data from crystals soaked with mercury. The apo form also crystallized in space group $P2_12_12_1$, and its structure was determined by the molecular replacement method using the

Received: November 14, 2011

Revised: December 30, 2011

Published: January 2, 2012



complex structure as a template. The final R_{factor} and R_{free} values are 0.159 and 0.205, respectively, for the complex and 0.210 and 0.261, respectively, for the apo form (SI Table). The overall structure of the mMDC1-FHA monomer exhibits the typical feature of the FHA domain, which folds into an 11-stranded β -sandwich that consists of two twisted β -sheets and several flexible loops (Figure 1B). In the complex structure, the hCHK2 peptide leans against a cleft formed by loops of mMDC1-FHA (L4, L6, and L10), and two protruding side chains (pThr68 and +3 Leu) of the hCHK2 peptide extend into two pockets provided by mMDC1-FHA. Similar to other FHA domains, the conserved Gly57 and His75 of mMDC1 interact with each other and possibly stabilize the architecture of the pThr-binding site. The binding between the mMDC1-FHA domain and the pThr68 peptide therefore buries $\sim 987 \text{ \AA}^2$ of solvent-accessible surface area.

The most unique feature of mMDC1-FHA (both the apo form and the complex) is that it forms a previously unreported dimeric structure. The only dimer reported previously is the segment-swapped crystal structure of CHFR-FHA, which however exists as a monomer in solution.¹¹ mMDC1-FHA remains as a stable dimer in solution [so does hMDC1-FHA (data not shown)] even under 4-fold protein dilution (from 2 to 0.5 mg/mL) or at a high salt concentration (450 mM NaCl) as evidenced by FPLC analysis (SI Figure 2). In the crystal structure, two mMDC1-FHA molecules approach each other in a head-to-tail but side-by-side orientation and wrap around each other with an interface of $\sim 1484 \text{ \AA}^2$. The biological implication regarding this unique dimerization is discussed separately in the SI Discussion. Close-up visualization of structures suggests that hydrogen bonds form between residues Asp125, Gln99, Lys102, Ser38, Gln129, and Arg35 of chain A and residues Lys102, Val101, Asp125, Arg35, and Ser38 of chain B (Figure

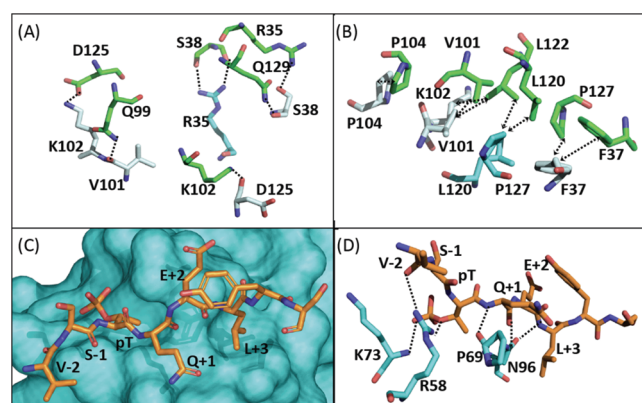


Figure 2. Interacting forces in the dimerization interface (A and B) and pThr binding interface (C and D). (A) Hydrogen bonds between the two chains illustrated as dashed lines. (B) van der Waals interactions between the two chains illustrated as two-headed dashed lines. (C) Binding pockets of mMDC1-FHA for accommodating the hCHK2-pThr68 peptide shown as a surface diagram. (D) Hydrogen bonds in the pThr binding interface illustrated as dashed lines (the electron density map showing key regions of interactions is shown in SI Figure 3). Chain A of mMDC1-FHA is colored green, chain B cyan, and hCHK2-pThr68 orange.

2A), while the van der Waals forces are maintained between residues Pro104, Val101, Leu122, Leu120, Pro127, and Phe37 of chain A and residues Pro104, Lys102, Val101, Leu120, Pro127, and Phe37 of chain B (Figure 2B).

We then analyzed the structure of the complex and found that the binding is supported by several hydrogen bonds between mMDC1-FHA and the pThr peptide, which shares a common feature with other FHA domains.^{12,13} Similar to Lys141 of CHK2-FHA,¹⁴ Lys73 of mMDC1-FHA interacts with the phosphate group of pThr68 using a hydrogen bond, but a notable difference is that Lys73 donates its main chain for interaction while Lys141 uses its side chain. Simultaneously, five hydrogen bonds are formed as shown in Figure 2D. Furthermore, two recessive pockets (one composed of Arg58, Pro69, Ser70, Ile71, Ser72, Leu95, and Asn96 and the other composed of Ser70, Asn96, Ala124, and Asp125, in which Ser70 and Asn96 are well conserved among FHA domains) accommodate two protruding side chains from pThr68 and +3 Leu, respectively (Figure 2C). This conformational fitness via two pockets presumably makes position +3 an important factor for the phosphopeptide sequence preference of mMDC1-FHA.^{12,13} Overall, binding of pThr68 induced relatively small conformational changes, except for small differences in loops L1, L3, L5, and L7, and several residues around the pThr binding pocket. In the SI Discussion, we have described detailed changes induced by the pThr peptide and also provided a detailed comparison among the FHA domains of MDC1, CHK2, and RNF8 (also in SI Figure 8).

A recent report showed that a phosphopeptide (SGSGSLA-FEEGpSQSTISS) derived from ATM autophosphorylation site Ser1981 is able to retrieve recombinant hMDC1-FHA, suggesting that an alternative phosphoserine binding capacity exists for MDC1-FHA,² a property never reported for any FHA domains. To examine the feasibility of pSer interaction, we replaced pThr68 with pSer in the complex structure and rebuilt the binding interface for comparison. In the pThr68 binding pocket mentioned above, a shallow groove formed by Ser70, Ser72, and Leu95 appears to accept the pThr γ -methyl group that forms a van der Waals interaction with the Leu95 side chain (Figure 3A). Although it seems that pSer can also fit into

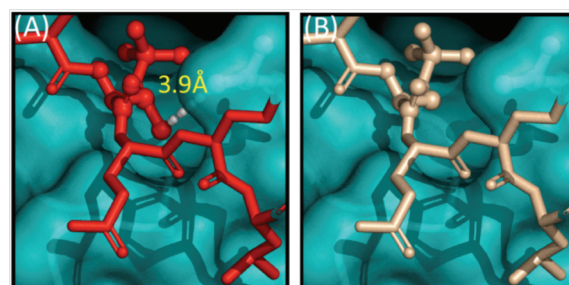


Figure 3. γ -Methyl group that stabilizes pThr binding. (A) Surface diagram showing that mMDC1-FHA forms a groove to accept the γ -methyl group of pThr68. The van der Waals force formed between Leu95 of FHA and the γ -methyl group of pThr68 is illustrated as a dashed line. (B) The same diagram except that pThr is replaced with pSer using Coot.

the pocket (Figure 3B), it is unable to make the key van der Waals force to stabilize the binding. Consistently, our ITC analysis showed that mMDC1-FHA binds the hCHK2-pThr68 peptide with a K_d of $40 \mu\text{M}$, while its binding with the ATM pSer1981 peptide was too weak to be detected (SI Figure 4). As controls, mMDC1-FHA was not able to bind to the non-phospho hCHK2-Thr68 peptide, nor can the R58A mutant of mMDC1-FHA bind to the pThr68 peptide (SI Figure 5). Although the possibility that the binding of pSer is just too

weak to be detected under the condition used may not be excluded, our result is in agreement with the general preference of pThr for FHA domains. The structural basis for the pThr preference has also been addressed recently.^{14,15}

A puzzling feature of the structure is that only one hCHK2-pThr68 peptide binds to each dimer. We cross-compared *Ca* atom groups in each of the two FHA chains using least-squares superposition and observed only marginal conformational differences among the four chains (rmsd of 0.32–0.37 Å), suggesting that the uneven binding is unlikely to be due to different binding specificities. We next superimposed the two monomers of the complex dimer to simulate the binding between the unbound mMDC1-FHA and the pThr68 peptide and then regenerated symmetry mates within 50 Å using PyMOL. The packing symmetry shows that Trp83, Asn84, and Lys85 of the unbound mMDC1-FHA monomer apparently overlap with neighboring +4 Tyr and +5 Ser of the pThr68 peptide, indicating a spatial limitation between the peptide and the unbound monomer (SI Figure 6). Thus, the uneven binding is most likely a crystal packing problem. Indeed, the binding stoichiometry between mMDC1-FHA and CHK2-pThr68 was estimated to be 1:1 in solution [the *N* value in the ITC analysis is 0.88 (SI Figure 4A)].

Finally, it has been reported recently that MDC1-FHA is phosphorylated at Thr98 by ATM, and that binding between MDC1-FHA and pThr98 mediates oligomerization of MDC1, leading to recruitment at the damage site and damage checkpoint activation.¹⁶ On the basis of the crystal structures reported above, Thr98 appears to be headed inward to the FHA structure that makes it almost inaccessible to ATM. However, we may not rule out the possibility that upon different ligand binding, the β 7 strand where Thr98 resides is able to rotate to allow Thr98 to be phosphorylated by ATM. This is possible because Thr98 is located at the beginning of β 7 that can potentially be affected by the flexibility of loop L6 (SI Figure 7). Further illustration and the possible mechanism of such conformational alteration are discussed in the SI Discussion. In this regard, how MDC1-FHA interacts with other binding partners is an important subject for future investigation. Past studies have demonstrated the structural and functional versatility of some FHA domains,^{12,13,17,18} and this work provides the first structural insight into the functionally diverse MDC1-FHA.

■ ASSOCIATED CONTENT

■ Supporting Information

SI Discussion, SI methods, SI Figures 1–8, SI Table, and list of abbreviations. This material is available free of charge via the Internet at <http://pubs.acs.org>.

Accession Codes

The Protein Data Bank entries for mMDC1-FHA without and with the hCHK2-pThr68 peptide are 3VA1 and 3VA4, respectively.

■ AUTHOR INFORMATION

Corresponding Author

*Phone: +86227855696-1013. E-mail: mdtsai@gate.sinica.edu.tw.

Author Contributions

H.-H.W. and P.-Y.W. contributed equally to this work.

■ ACKNOWLEDGMENTS

National Health Research Institute and Academia Sinica, Taiwan. Synchrotron radiation beamline 13B1 (NSRRC, HsinChu, Taiwan) and beamline 12B2 (Spring-8, Hyogo, Japan).

■ REFERENCES

- (1) Lou, Z., Minter-Dykhouse, K., Franco, S., Gostissa, M., Rivera, M. A., Celeste, A., Manis, J. P., van Deursen, J., Nussenzweig, A., Paull, T. T., Alt, F. W., and Chen, J. (2006) *Mol. Cell* 21, 187–200.
- (2) So, S., Davis, A. J., and Chen, D. J. (2009) *J. Cell Biol.* 187, 977–990.
- (3) Jungmichel, S., and Stucki, M. (2010) *Chromosoma* 119, 337–349.
- (4) Durocher, D., Taylor, I. A., Sarbassova, D., Haire, L. F., Westcott, S. L., Jackson, S. P., Smerdon, S. J., and Yaffe, M. B. (2000) *Mol. Cell* 6, 1169–1182.
- (5) Lou, Z., Minter-Dykhouse, K., Wu, X., and Chen, J. (2003) *Nature* 421, 957–961.
- (6) Lukas, C., Falck, J., Bartkova, J., Bartek, J., and Lukas, J. (2003) *Nat. Cell Biol.* 5, 255–260.
- (7) Wu, L., Luo, K., Lou, Z., and Chen, J. (2008) *Proc. Natl. Acad. Sci. U.S.A.* 105, 11200–11205.
- (8) Spycher, C., Miller, E. S., Townsend, K., Pavic, L., Morrice, N. A., Janscak, P., Stewart, G. S., and Stucki, M. (2008) *J. Cell Biol.* 181, 227–240.
- (9) Chapman, J. R., and Jackson, S. P. (2008) *EMBO Rep.* 9, 795–801.
- (10) Huen, M. S., Grant, R., Manke, I., Minn, K., Yu, X., Yaffe, M. B., and Chen, J. (2007) *Cell* 131, 901–914.
- (11) Stavridi, E. S., Huyen, Y., Loreto, I. R., Scolnick, D. M., Halazonetis, T. D., Pavletich, N. P., and Jeffrey, P. D. (2002) *Structure* 10, 891–899.
- (12) Mahajan, A., Yuan, C., Lee, H., Chen, E. S., Wu, P. Y., and Tsai, M. D. (2008) *Sci. Signaling* 1, re12.
- (13) Liang, X., and Van Doren, S. R. (2008) *Acc. Chem. Res.* 41, 991–999.
- (14) Li, J., Williams, B. L., Haire, L. F., Goldberg, M., Wilker, E., Durocher, D., Yaffe, M. B., Jackson, S. P., and Smerdon, S. J. (2002) *Mol. Cell* 9, 1045–1054.
- (15) Pennell, S., Westcott, S., Ortiz-Lombardia, M., Patel, D., Li, J., Nott, T. J., Mohammed, D., Buxton, R. S., Yaffe, M. B., Verma, C., and Smerdon, S. J. (2010) *Structure* 18, 1587–1595.
- (16) Luo, K., Yuan, J., and Lou, Z. (2011) *J. Biol. Chem.* 286, 28192–28199.
- (17) Lee, H., Yuan, C., Hammet, A., Mahajan, A., Chen, E. S., Wu, M. R., Su, M. I., Heierhorst, J., and Tsai, M. D. (2008) *Mol. Cell* 30, 767–778.
- (18) Byeon, I. J., Li, H., Song, H., Gronenborn, A. M., and Tsai, M. D. (2005) *Nat. Struct. Mol. Biol.* 12, 987–993.